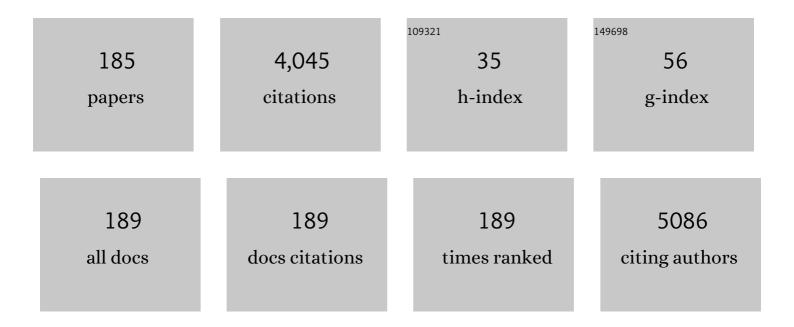
## Yoshiyuki Yamashita

List of Publications by Year in descending order

Source: https://exaly.com/author-pdf/7657457/publications.pdf Version: 2024-02-01



#	ARTICLE	IF	CITATIONS
1	Heusler compounds CoFeMn mml:math xmlns:mml="http://www.w3.org/1998/Math/MathML" display="inline"> <mml:mi>Z</mml:mi> ( <mml:math) 0.784314="" 1="" 10="" 50="" 7<="" etqq1="" overlock="" rgbt="" td="" tf="" tj=""><td>742 Td (xn 3.2</td><td>ulns:mml='l 221</td></mml:math)>	742 Td (xn 3.2	ulns:mml='l 221
2	Formation of Ni <sub>3</sub> C Nanocrystals by Thermolysis of Nickel Acetylacetonate in Oleylamine: Characterization Using Hard X-ray Photoelectron Spectroscopy. Chemistry of Materials, 2008, 20, 4156-4160.	6.7	162
3	Probing bulk electronic structure with hard X-ray angle-resolved photoemission. Nature Materials, 2011, 10, 759-764.	27.5	153
4	Present Status of the NIMS Contract Beamline BL15XU at SPring-8. AIP Conference Proceedings, 2010, , .	0.4	127
5	Bulk electronic structure of the dilute magnetic semiconductor Ga1â^'xMnxAs through hard X-ray angle-resolved photoemission. Nature Materials, 2012, 11, 957-962.	27.5	117
6	X-ray photoemission spectroscopy analysis of N-containing carbon-based cathode catalysts for polymer electrolyte fuel cells. Journal of Power Sources, 2011, 196, 1006-1011.	7.8	98
7	Formation of a K—In—Se Surface Species by NaF/KF Postdeposition Treatment of Cu(In,Ga)Se <sub>2</sub> Thin-Film Solar Cell Absorbers. ACS Applied Materials & Interfaces, 2017, 9, 3581-3589.	8.0	94
8	Band bending and surface defects in <i><math>\hat{l}^2</math></i> -Ga2O3. Applied Physics Letters, 2012, 100, .	3.3	82
9	<i>In Situ</i> Tuning of Magnetization and Magnetoresistance in Fe <sub>3</sub> O <sub>4</sub> Thin Film Achieved with All-Solid-State Redox Device. ACS Nano, 2016, 10, 1655-1661.	14.6	80
10	Model forCdefect on Si(100):â€,â€,The dissociative adsorption of a single water molecule on two adjacent dimers. Physical Review B, 2003, 67, .	3.2	77
11	Sulfur Modification of Au via Treatment with Piranha Solution Provides Low-Pd Releasing and Recyclable Pd Material, SAPd. Journal of the American Chemical Society, 2010, 132, 7270-7272.	13.7	77
12	Activity of oxygen reduction reaction on small amount of amorphous CeO promoted Pt cathode for fuel cell application. Electrochimica Acta, 2011, 56, 3874-3883.	5.2	75
13	Interface properties of magnetic tunnel junction <mml:math xmlns:mml="http://www.w3.org/1998/Math/MathML" display="inline"&gt;<mml:mrow><mml:mrow><mml:mtext>La</mml:mtext></mml:mrow><mml:mrow> Physical Review B. 2010. 82</mml:mrow></mml:mrow></mml:math 	> < <sup>3</sup> tîml:mn	>70 <sup>1</sup> 7
14	Depletion of the In2O3(001) and (111) surface electron accumulation by an oxygen plasma surface treatment. Applied Physics Letters, 2011, 98, .	3.3	71
15	Electronic Structure Changes across the Metamagnetic Transition in FeRh via Hard X-Ray Photoemission. Physical Review Letters, 2012, 108, 257208.	7.8	68
16	Observation of boron diffusion in an annealed Ta/CoFeB/MgO magnetic tunnel junction with standing-wave hard x-ray photoemission. Applied Physics Letters, 2012, 101, .	3.3	64
17	Oxygen migration at Pt/HfO2/Pt interface under bias operation. Applied Physics Letters, 2010, 97, .	3.3	59
18	Studies on interface states at ultrathin SiO2/Si(100) interfaces by means of x-ray photoelectron spectroscopy under biases and their passivation by cyanide treatment. Journal of Applied Physics, 1998, 83, 2098-2103.	2.5	57

#	Article	IF	CITATIONS
19	Spectroscopic observation of interface states of ultrathin silicon oxide. Journal of Applied Physics, 1996, 79, 7051-7057.	2.5	56
20	Electronic and crystallographic structure, hard x-ray photoemission, and mechanical and transport properties of the half-metallic Heusler compound Co <mml:math xmlns:mml="http://www.w3.org/1998/Math/MathML" display="inline"&gt;<mml:msub><mml:mrow /&gt;<mml:mn>2</mml:mn></mml:mrow </mml:msub>MnGe. Physical Review B, 2011, 84, .</mml:math 	3.2	56
21	Bias application hard x-ray photoelectron spectroscopy study of forming process of Cu/HfO2/Pt resistive random access memory structure. Applied Physics Letters, 2011, 99, .	3.3	56
22	Precursor Mediated Cycloaddition Reaction of Ethylene to the Si(100)c(4 × 2) Surface. Journal of the American Chemical Society, 2004, 126, 9922-9923.	13.7	55
23	Ground state of the Si(001) surface revisited?is seeing believing?. Progress in Surface Science, 2004, 76, 147-162.	8.3	47
24	Detection of the valence band in buried Co2MnSi–MgO tunnel junctions by means of photoemission spectroscopy. Applied Physics Letters, 2008, 92, .	3.3	46
25	Chemical insight into electroforming of resistive switching manganite heterostructures. Nanoscale, 2013, 5, 3954.	5.6	44
26	Dependence of interface states in the Si band gap on oxide atomic density and interfacial roughness. Physical Review B, 1999, 59, 15872-15881.	3.2	43
27	Lateral Displacement by Transient Mobility in Chemisorption of CO on Pt(997). Physical Review Letters, 2003, 90, 248301.	7.8	43
28	Microscopic observation of precursor-mediated adsorption process ofNH3onSi(100)c(4×2)using STM. Physical Review B, 2003, 68, .	3.2	41
29	Bonding and Structure of 1,4-Cyclohexadiene Chemisorbed on Si(100)(2×1). Journal of Physical Chemistry B, 2001, 105, 3718-3723.	2.6	40
30	Chemical nature of nanostructures of La0.6Sr0.4MnO3 on SrTiO3(100). Surface Science, 2002, 514, 54-59.	1.9	40
31	Adsorption state of 1,4-cyclohexadiene onSi(100)(2×1). Physical Review B, 2000, 62, 7576-7580.	3.2	39
32	Water Adsorption on Rh(111) at 20 K:Â From Monomer to Bulk Amorphous Ice. Journal of Physical Chemistry B, 2005, 109, 5816-5823.	2.6	38
33	XPS study of Sb-/In-doping and surface pinning effects on the Fermi level in SnO2 (101) thin films. Applied Physics Letters, 2011, 98, .	3.3	38
34	Role of residual transition-metal atoms in oxygen reduction reaction in cobalt phthalocyanine-based carbon cathode catalysts for polymer electrolyte fuel cell. Journal of Power Sources, 2011, 196, 8346-8351.	7.8	38
35	Identifying the Electronic Character and Role of the Mn States in the Valence Band of (Ga,Mn)As. Physical Review Letters, 2013, 111, 097201.	7.8	36
36	Insulating state of ultrathin epitaxial LaNiO <mml:math xmlns:mml="http://www.w3.org/1998/Math/MathML" display="inline"&gt;<mml:msub><mml:mrow /&gt;<mml:mn>3</mml:mn></mml:mrow </mml:msub>thin films detected by hard x-ray photoemission. Physical Review B, 2011, 84, .</mml:math 	3.2	35

Υοςηιγυκι Υαμασηιτά

#	Article	IF	CITATIONS
37	Interface chemistry of pristine TiN/La:Hf0.5Zr0.5O2 capacitors. Applied Physics Letters, 2020, 116, .	3.3	35
38	Interface states at ultrathin oxide/Si(111) interfaces obtained from xâ€ray photoelectron spectroscopy measurements under biases. Applied Physics Letters, 1996, 69, 2276-2278.	3.3	33
39	The first layer of water on Rh(111): Microscopic structure and desorption kinetics. Journal of Chemical Physics, 2006, 125, 054717.	3.0	33
40	Au <sup>+</sup> and Au <sup>3+</sup> ions in CeO <sub>2</sub> rf-sputtered thin films. Journal Physics D: Applied Physics, 2009, 42, 115301.	2.8	32
41	Polarity-dependent photoemission spectra of wurtzite-type zinc oxide. Applied Physics Letters, 2012, 100, .	3.3	32
42	Direct observation of site-specific valence electronic structure at theSiO2â^•Siinterface. Physical Review B, 2006, 73, .	3.2	31
43	NbPt <sub>3</sub> Intermetallic Nanoparticles: Highly Stable and COâ€Tolerant Electrocatalyst for Fuel Oxidation. ChemElectroChem, 2014, 1, 728-732.	3.4	31
44	Determination of Schottky barrier profile at Pt/SrTiO3:Nb junction by x-ray photoemission. Applied Physics Letters, 2012, 101, .	3.3	27
45	Highly Selective Surface Lewis Acidâ^'Base Reaction: Trimethylamine on Si(100)c(4×2). Journal of Physical Chemistry B, 2004, 108, 4737-4742.	2.6	26
46	Methods of observation and elimination of semiconductor defect states. Solar Energy, 2006, 80, 645-652.	6.1	26
47	Interface States for Si-Based MOS Devices with an Ultrathin Oxide Layer: X-Ray Photoelectron Spectroscopic Measurements under Biases. Japanese Journal of Applied Physics, 1995, 34, 959-964.	1.5	25
48	Energy distribution of surface states in the Si band-gap for MOS diodes obtained from XPS measurements under biases. Surface Science, 1995, 326, 124-132.	1.9	25
49	The growth process of first water layer and crystalline ice on the Rh(111) surface. Journal of Chemical Physics, 2009, 130, 034706.	3.0	25
50	Energy-level alignments and photo-induced carrier processes at the heteromolecular interface of quaterrylene and N,N′-dioctyl-3,4,9,10-perylenedicarboximide. Physical Chemistry Chemical Physics, 2011, 13, 6280.	2.8	25
51	Electronic structure of delta-doped La:SrTiO <sub>3</sub> layers by hard x-ray photoelectron spectroscopy. Applied Physics Letters, 2012, 100, 261603.	3.3	25
52	Purely Site-Specific Chemisorption and Conformation of Trimethylamine on Si(100)c(4 × 2). Journal of the American Chemical Society, 2003, 125, 9252-9253.	13.7	24
53	Development of a Recyclable and Low‣eaching Palladium Catalyst Supported on Sulfurâ€Modified Gallium Arsenideâ€(001) for Use in Suzuki–Miyaura Coupling. ChemCatChem, 2009, 1, 279-285.	3.7	24
54	Identification of Different Electron Screening Behavior Between the Bulk and Surface of (Ga,Mn)As. Physical Review Letters, 2011, 107, 187203.	7.8	24

Υοςηιγικι Υαμασηιτά

#	Article	IF	CITATIONS
55	Photoelectron spectroscopic study of band alignment of polymer/ZnO photovoltaic device structure. Applied Physics Letters, 2013, 102, .	3.3	24
56	Determination of the input parameters for inelastic background analysis combined with HAXPES using a reference sample. Applied Surface Science, 2018, 432, 60-70.	6.1	24
57	The Precursor Mediated Chemisorption of Vinyl Bromide on Si(100)c(4×2). Journal of Physical Chemistry B, 2004, 108, 5703-5708.	2.6	22
58	Adsorption states of NO on the Pt(111) step surface. Surface Science, 2006, 600, 3477-3483.	1.9	22
59	Thermoelectric properties and electronic structure of substituted Heusler compounds: NiTi0.3â^'xScxZr0.35Hf0.35Sn. Applied Physics Letters, 2010, 97, .	3.3	22
60	Characterization of Surface Structure Evolution in Ni <sub>3</sub> Al Foil Catalysts by Hard X-ray Photoelectron Spectroscopy. Journal of Physical Chemistry C, 2010, 114, 6047-6053.	3.1	22
61	Quantitative determination of elemental diffusion from deeply buried layers by photoelectron spectroscopy. Journal of Applied Physics, 2018, 124, .	2.5	22
62	Electronic and Vibrational States of Cyclopentene on Si(100)(2×1). Journal of Physical Chemistry B, 2002, 106, 1691-1696.	2.6	21
63	Nature of interface bonding of ethylene and benzene with Si(100)c(4×2): angle-dependent Si2p high resolution photoelectron spectroscopy studies. Surface Science, 2002, 513, 413-421.	1.9	21
64	Hard x-ray photoelectron spectroscopy study on band alignment at poly(3,4-ethylenedioxythiophene):poly(styrenesulfonate)/ZnO interface. Applied Physics Letters, 2012, 101, .	3.3	21
65	Direct observation of redox state modulation at carbon/amorphous tantalum oxide thin film hetero-interface probed by means of in situ hard X-ray photoemission spectroscopy. Solid State Ionics, 2013, 253, 110-118.	2.7	21
66	Room temperature redox reaction by oxide ion migration at carbon/Gd-doped CeO <sub>2</sub> heterointerface probed by an <i>in situ</i> hard x-ray photoemission and soft x-ray absorption spectroscopies. Science and Technology of Advanced Materials, 2013, 14, 045001.	6.1	21
67	High resolution Si 2p photoelectron spectroscopy of unsaturated hydrocarbon molecules adsorbed on Si(100)c(4×2): the interface bonding and charge transfer between the molecule and the Si substrate. Journal of Electron Spectroscopy and Related Phenomena, 2001, 114-116, 389-393.	1.7	20
68	Direct Evidence for Asymmetric Dimer on Si(100) at Low Temperature by Means of High-Resolution Si 2p Photoelectron Spectroscopy. Japanese Journal of Applied Physics, 2002, 41, L272-L274.	1.5	20
69	Adsorbed states of cyclopentene, cyclohexene, and 1,4-cyclohexadiene on Si(1 0 0)(2×1): towards the fabrication of novel organic films/Si hybrid structures. Applied Surface Science, 2001, 169-170, 172-175.	6.1	19
70	Bias-voltage application in a hard x-ray photoelectron spectroscopic study of the interface states at oxide/Si(100) interfaces. Journal of Applied Physics, 2013, 113, .	2.5	19
71	Reaction mechanism and adsorbed states of cyclohexene on Si(100)(2×1). Journal of Electron Spectroscopy and Related Phenomena, 2001, 114-116, 383-387.	1.7	18
72	Method of observation of low density interface states by means of X-ray photoelectron spectroscopy under bias and passivation by cyanide ions. Applied Surface Science, 2006, 252, 7700-7712.	6.1	18

Υοςηιγικι Υαμασηιτα

#	Article	IF	CITATIONS
73	Interface structure and the chemical states of Pt film on polar-ZnO single crystal. Applied Physics Letters, 2009, 94, 221904.	3.3	18
74	Hard x-ray photoelectron spectroscopy of buried Heusler compounds. Journal Physics D: Applied Physics, 2009, 42, 084010.	2.8	18
75	Defects in ZnO transparent conductors studied by capacitance transients at ZnO/Si interface. Applied Physics Letters, 2011, 98, 082101.	3.3	18
76	Systematic investigation of surface and bulk electronic structure of undoped In-polar InN epilayers by hard X-ray photoelectron spectroscopy. Journal of Applied Physics, 2013, 114, .	2.5	17
77	Interface stateâ€induced shift of the oxide and semiconductor core levels for metal–oxide–semiconductor devices. Journal of Applied Physics, 1996, 80, 1578-1582.	2.5	15
78	Microscopic adsorption process of CO onSi(100)c(4×2)by means of low-temperature scanning tunneling microscopy. Physical Review B, 2003, 68, .	3.2	15
79	Bias-voltage Application in Hard X-Ray Photoelectron Spectroscopy for Characterization of Advanced Materials. E-Journal of Surface Science and Nanotechnology, 2010, 8, 81-83.	0.4	15
80	Selective functionalization of the Si(100) surface by switching the adsorption linkage of a bifunctional organic molecule. Chemical Physics Letters, 2004, 388, 27-30.	2.6	14
81	Low-energy electron-stimulated chemical reactions of CO in water ice. Chemical Physics Letters, 2004, 388, 384-388.	2.6	14
82	Pt and Sn Doped Sputtered CeO <sub>2</sub> Electrodes for Fuel Cell Applications. Fuel Cells, 2010, 10, 139-144.	2.4	14
83	Intermolecular interaction and arrangements of adsorbed 1,4-cyclohexadiene molecules on Si()(2×1). Surface Science, 2003, 531, 199-207.	1.9	13
84	Hard x-ray photoemission study of near-Heusler FexSi1â^'xalloys. Physical Review B, 2011, 83, .	3.2	13
85	A new method for the growth of silicon oxide layers below 300°C by use of catalytic activity of platinum overlayers. Applied Surface Science, 1997, 108, 433-438.	6.1	12
86	Structural and chemical property of unsaturated cyclic-hydrocarbon molecules regularly chemisorbed on Si(0 0 1) surface. Applied Surface Science, 2004, 234, 162-167.	6.1	12
87	Nondestructive characterization of a TiN metal gate: Chemical and structural properties by means of standing-wave hard x-ray photoemission spectroscopy. Journal of Applied Physics, 2012, 112, .	2.5	12
88	Adsorption States and Dissociation Processes of Oxygen Molecules on Cu(100) at Low Temperature. Journal of Physical Chemistry C, 2007, 111, 15059-15063.	3.1	11
89	Conduction-band electronic states of YbInCu <mml:math xmlns:mml="http://www.w3.org/1998/Math/MathML" display="inline"&gt;<mml:msub><mml:mrow /&gt;<mml:mn>4</mml:mn></mml:mrow </mml:msub>studied by photoemission and soft x-ray absorption spectroscopies. Physical Review B. 2011. 84.</mml:math 	3.2	11
90	Direct Spectroscopic Evidence of Bias-Induced Shifts of Semiconductor Band Edges for Metal-Insulator-Semiconductor Diodes. Japanese Journal of Applied Physics, 1994, 33, L754-L756.	1.5	10

Υοςηιγικι Υαμασηιτα

#	Article	IF	CITATIONS
91	Coverage-dependent sticking probability and desorption kinetics of water molecules on Rh(111). Journal of Chemical Physics, 2008, 129, 016101.	3.0	10
92	Smart Decoration of Mesoporous TiO <sub>2</sub> Nanospheres with Noble Metal Alloy Nanoparticles into Core–Shell, Yolk–Core–Shell, and Surfaceâ€Đispersion Morphologies. European Journal of Inorganic Chemistry, 2014, 2014, 4254-4257.	2.0	10
93	Vibrational structure in C 1s photoelectron spectra of ethylene on the Si(100)(2×1) surface. Chemical Physics Letters, 2003, 374, 476-481.	2.6	9
94	Transient diffusion and cluster formation of water molecules on Rh(111) at 20K. Journal of Chemical Physics, 2007, 126, 141102.	3.0	9
95	Electron Transport Properties and Dielectric Breakdown of Alkyl Monolayers Chemisorbed on a Highly Doped n-Type Si(111) Surface. Japanese Journal of Applied Physics, 2009, 48, 055003.	1.5	9
96	Hard x-ray photoemission spectroscopic investigation of palladium catalysts immobilized on a GaAs(001) surface. Journal of Applied Physics, 2010, 108, .	2.5	9
97	Structural analysis and electrical properties of pure Ge3N4 dielectric layers formed by an atmospheric-pressure nitrogen plasma. Journal of Applied Physics, 2011, 110, 064103.	2.5	9
98	Post-synthesis dispersion of metal nanoparticles by poly(amidoamine) dendrimers: size-selective inclusion, water solubilization, and improved catalytic performance. Chemical Communications, 2012, 48, 7441.	4.1	9
99	Photoelectron spectroscopic study of electronic state and surface structure of In2O3 single crystals. Applied Physics Express, 2017, 10, 011102.	2.4	9
100	Forming mechanism of Te-based conductive-bridge memories. Applied Surface Science, 2018, 432, 34-40.	6.1	9
101	Relationship between electrical properties and interface structures of SiO2/4H-SiC prepared by dry and wet oxidation. AIP Advances, 2019, 9, .	1.3	9
102	Compact UHV system for fabrication and in situ analysis of electron beam deposited structures using a focused low energy electron beam. Review of Scientific Instruments, 2006, 77, 053702.	1.3	8
103	Search for adsorption potential energy minima of NO on Pt(997) at 11K. Surface Science, 2006, 600, 3560-3563.	1.9	8
104	Impact of Mg concentration on energy-band-depth profile of Mg-doped InN epilayers analyzed by hard X-ray photoelectron spectroscopy. Applied Physics Letters, 2013, 103, .	3.3	8
105	Investigation of the near-surface structures of polar InN films by chemical-state-discriminated hard X-ray photoelectron diffraction. Applied Physics Letters, 2013, 102, .	3.3	8
106	Ge incorporated epitaxy of (110) rutile TiO2 on (100) Ge single crystal at low temperature by pulsed laser deposition. Thin Solid Films, 2015, 591, 105-110.	1.8	8
107	Characterization of 'metal resist' for EUV lithography. Proceedings of SPIE, 2016, , .	0.8	8
108	Effects of interface roughness on the density of interface states at ultrathin oxide/Si interfaces: XPS measurements under biases. Applied Surface Science, 1997, 117-118, 176-180.	6.1	7

#	Article	IF	CITATIONS
109	Regioselective Cycloaddition Reaction of Alkene Molecules with the Asymmetric Dimer on Si(100)c(4×2). Journal of the American Chemical Society, 2007, 129, 1242-1245.	13.7	7
110	X-dependent electronic structure of YbXCu4 (X=Cd, In, Sn) investigated by hard X-ray photoemission spectroscopy. Journal of Electron Spectroscopy and Related Phenomena, 2011, 184, 203-206.	1.7	7
111	Temperature-Induced Valence Transition of EuPd <sub>2</sub> Si <sub>2</sub> Studied by Hard X-ray Photoelectron Spectroscopy. Japanese Journal of Applied Physics, 2011, 50, 05FD03.	1.5	7
112	Observation of filament formation process of Cu/HfO <sub>2</sub> /Pt ReRAM structure by hard x-ray photoelectron spectroscopy under bias operation. Journal of Materials Research, 2012, 27, 869-878.	2.6	7
113	Hard x-ray photoelectron spectroscopy study of Ge2Sb2Te5; as-deposited amorphous, crystalline, and laser-reamorphized. Applied Physics Letters, 2014, 104, 061909.	3.3	7
114	Photoelectron spectroscopic study of electronic states and surface structure of an in situ cleaved In2O3 (111) single crystal. Japanese Journal of Applied Physics, 2019, 58, SDDG06.	1.5	7
115	Residual gas effects on high-resolution Si2p spectra of Si(100)c(4×2). Surface Science, 2004, 566-568, 467-470.	1.9	6
116	Heat Transport Analysis of Femtosecond Laser Ablation with Full Lagrangian Modified Molecular Dynamics. International Journal of Thermophysics, 2006, 27, 627-646.	2.1	6
117	Fabrication and analysis of buried iron silicide microstructures using a focused low energy electron beam. Surface Science, 2007, 601, 5108-5111.	1.9	6
118	Microscopic diffusion processes of NO on the Pt(997) surface. Journal of Chemical Physics, 2008, 128, 054701.	3.0	6
119	Schottky barrier height behavior of Pt–Ru alloy contacts on single-crystal n-ZnO. Journal of Applied Physics, 2010, 107, .	2.5	6
120	Delta-doped epitaxial La:SrTiO3 field-effect transistor. Applied Physics Letters, 2011, 98, 242113.	3.3	6
121	Strong Correlation Between Oxygen Donor and Near-Surface Electron Accumulation in Undoped and Mg-Doped In-Polar InN Films. Applied Physics Express, 2012, 5, 031002.	2.4	6
122	Hydroxylated surface of GaAs as a scaffold for a heterogeneous Pd catalyst. Physical Chemistry Chemical Physics, 2012, 14, 1424-1430.	2.8	6
123	Photoelectron spectroscopic study on electronic state and electrical properties of SnO2 single crystals. Japanese Journal of Applied Physics, 2019, 58, 080903.	1.5	6
124	Interface states in the Si band-gap obtained from XPS measurements under biases. Surface Science, 1996, 357-358, 455-458.	1.9	5
125	Soft X-Ray Absorption and Emission Study of Silicon Oxynitride/Si(100) Interface. Japanese Journal of Applied Physics, 2007, 46, L77-L79.	1.5	5
126	Surface and bulk electronic structures of heavily Mg-doped InN epilayer by hard X-ray photoelectron spectroscopy. Journal of Applied Physics, 2017, 121, .	2.5	5

Υοςηιγυκι Υαμασηιτά

#	Article	IF	CITATIONS
127	Evaluation of Band Alignment of SrNbO <sub>2</sub> N Using Hard X-ray Photoelectron Spectroscopy. Journal of Physical Chemistry C, 2020, 124, 5528-5532.	3.1	5
128	Unraveling the Resistive Switching Mechanisms in LaMnO <sub>3+δ</sub> -Based Memristive Devices by <i>Operando</i> Hard X-ray Photoemission Measurements. ACS Applied Electronic Materials, 2021, 3, 5555-5562.	4.3	5
129	Real-space observation of local anisotropic correlation between buckled dimers on Si(100) induced by a bidentate adsorbed molecule. Chemical Communications, 2011, 47, 10392.	4.1	4
130	(Invited) Direct Observation of Electronic States in Gate Stack Structures: XPS under Device Operation. ECS Transactions, 2011, 41, 331-336.	0.5	4
131	New Direct Spectroscopic Method for Determination of Bias-Dependent Electronic States: Hard X-ray Photoelectron Spectroscopy Under Device Operation. Japanese Journal of Applied Physics, 2013, 52, 108005.	1.5	4
132	Reaction mechanism of ZrO <i> <sub>x</sub> </i> metal resists with extreme ultraviolet irradiation. Japanese Journal of Applied Physics, 2019, 58, SDDC01.	1.5	4
133	Relationship between band-offset, gate leakage current, and interface states density at SiO2/4H-SiC (000-1) interface. AIP Advances, 2019, 9, 045002.	1.3	4
134	Photoelectron spectroscopic study on electronic state of corundum In2O3 epitaxial thin film grown by mist-CVD. Japanese Journal of Applied Physics, 2020, 59, SIIG12.	1.5	4
135	Atomic Structures and Chemical States of Active and Inactive Dopant Sites in Si-Doped GaN. ACS Applied Electronic Materials, 2021, 3, 4618-4622.	4.3	4
136	Electronic states and chemical reactivity of Si(100)c(4×2) surface at low temperature studied by high resolution Si 2p core level photoelectron spectroscopy. Surface Science, 2003, 532-535, 716-720.	1.9	3
137	Analysis of ITO/Mg:GaN interfaces by synchrotron radiation hard X-ray photoemission spectroscopy and their electrical characteristics. Applied Surface Science, 2008, 255, 2149-2152.	6.1	3
138	Sulfur-mediated palladium catalyst immobilized on a GaAs surface. Journal of Applied Physics, 2012, 111, 124908.	2.5	3
139	Direct observation of bias-dependence potential distribution in metal/HfO2 gate stack structures by hard x-ray photoelectron spectroscopy under device operation. Journal of Applied Physics, 2014, 115, 043721.	2.5	3
140	Photoelectron spectroscopic study on band alignment of poly(3-hexylthiophene-2,5-diyl)/polar-ZnO heterointerface. Thin Solid Films, 2014, 554, 194-198.	1.8	3
141	Formation of Amorphous Pt Oxides: Characterization and Their Catalysis. Materials Transactions, 2015, 56, 490-494.	1.2	3
142	Bias induced Cu ion migration behavior in resistive change memory structure observed by hard X-ray photoelectron spectroscopy. Japanese Journal of Applied Physics, 2015, 54, 06FG01.	1.5	3
143	Effect of Y and Mn doping into rutile type TiO2/Ge stack structure by combinatorial synthesis. Japanese Journal of Applied Physics, 2017, 56, 06GF11.	1.5	3
144	Experimental and theoretical studies on atomic structures of the interface states at SiO2/4H-SiC(0001) interface. Journal of Applied Physics, 2022, 131, .	2.5	3

Υοςηιγικι Υαμασηιτά

#	Article	IF	CITATIONS
145	Multi-stage Decoding For Multi-level Block Modulation Codes And Its Performance Analysis. , 0, , .		2
146	Adsorbed states of 1,1,1-trifluoro-2-propanol on Si(100). Surface Science, 2003, 529, 288-294.	1.9	2
147	Effects of interface roughness on the local valence electronic structure at the SiO2/Si interface: Soft X-ray absorption andÂemission study. European Physical Journal Special Topics, 2006, 132, 259-262.	0.2	2
148	Direct observation of the site-specific valence electronic structure at SiO2/Si(111) interface. E-Journal of Surface Science and Nanotechnology, 2006, 4, 280-284.	0.4	2
149	Degradation of reliability of high-k gate dielectrics caused by point defects and residual stress. , 2008, , .		2
150	Low-Temperature STM and UPS Study of Adsorption States of 1,4-Cyclohexadiene on Si(100)c(4×2). Journal of Physical Chemistry C, 2008, 112, 15009-15014.	3.1	2
151	Low-Temperature Surface Photochemistry of π-bonded Ethylene on Si(100) <i>c</i> (4×2). Japanese Journal of Applied Physics, 2009, 48, 08JB14.	1.5	2
152	Effect of near atmospheric pressure nitrogen plasma treatment on Pt/ZnO interface. Journal of Applied Physics, 2012, 112, .	2.5	2
153	Investigation of the Effect of Oxygen on the Near-Surface Electron Accumulation in Nonpolar m-Plane (101̄O) InN Film by Hard X-ray Photoelectron Spectroscopy. Japanese Journal of Applied Physics, 2013, 52, 08JD01.	1.5	2
154	Thin-film growth of (110) rutile TiO2on (100) Ge substrate by pulsed laser deposition. Japanese Journal of Applied Physics, 2016, 55, 06GG06.	1.5	2
155	Spectroscopic Observation of the Interface States at the SiO <sub>2</sub> /4H-SiC(0001) Interface. E-Journal of Surface Science and Nanotechnology, 2019, 17, 56-60.	0.4	2
156	Band alignment at non-polar AlN/MnS interface investigated by hard X-ray photoelectron spectroscopy. Japanese Journal of Applied Physics, 2020, 59, SIIG07.	1.5	2
157	Direct Observation of Valence and Conduction States near the SiO2/Si(100) Interface. E-Journal of Surface Science and Nanotechnology, 2008, 6, 209-212.	0.4	2
158	CYCLOADDITION REACTION BETWEEN ORGANIC MOLECULES AND Si(100) AND ELECTRONIC PROPERTIES OF ADSORBED MOLECULES. International Journal of Nanoscience, 2007, 06, 95-102.	0.7	1
159	Degradation of interface integrity between a high-k dielectric thin film and a gate electrode due to excess oxygen in the film. , 2009, , .		1
160	Bias dependent potential distribution of a Pt/HfO <sub>2</sub> /SiO <sub>2</sub> /Si gate structure obtained from a bias application in hard X-ray photoelectron spectroscopy. Japanese Journal of Applied Physics, 2014, 53, 05FH05.	1.5	1
161	Electronic structure of the polymer-cathode interface of an organic electroluminescent device investigated using operando hard x-ray photoelectron spectroscopy. Journal of Applied Physics, 2015, 118, 085308.	2.5	1
162	Bottom-electrode effect on switching behavior and interface reaction in nanoionic-based resistive changing memory. Japanese Journal of Applied Physics, 2016, 55, 08PC03.	1.5	1

#	Article	IF	CITATIONS
163	Surface and bulk electronic structures of unintentionally and Mg-doped In0.7Ga0.3N epilayer by hard X-ray photoelectron spectroscopy. Journal of Applied Physics, 2018, 123, 095701.	2.5	1
164	Origin of Fermi level pinning in high-k gate stack structures studied by operando hard x-ray photoelectron spectroscopy. Journal of Electron Spectroscopy and Related Phenomena, 2020, 238, 146890.	1.7	1
165	Determination of Band Structures of InN/GaN Interfaces by Synchrotron Radiation Hard X-ray Photoemission Spectroscopy. E-Journal of Surface Science and Nanotechnology, 2008, 6, 254-257.	0.4	1
166	Site-specific Observation of the Valence Electronic Structure at SiO2/Si Interface by Means of Soft X-ray Absorption and Emission Spectroscopy. Hyomen Kagaku, 2005, 26, 514-517.	0.0	1
167	Interface stability of electrode/Bi-containing relaxor ferroelectric oxide for high-temperature operational capacitor. Japanese Journal of Applied Physics, 2016, 55, 06GJ12.	1.5	1
168	New direct spectroscopic method for determination of the energy distribution of interface states. , 0, , $\cdot$		0
169	ELECTRONIC STRUCTURES OF NAKED AND MOLECULAR ENCAPSULATED <font>Au</font> NANOPARTICLES. International Journal of Nanoscience, 2009, 08, 181-184.	0.7	0
170	Wet Chemical Synthesis of Ni-Al Nanoparticles at Ambient Condition. Advanced Materials Research, 2012, 557-559, 442-447.	0.3	0
171	(Invited) Photoelectron Spectroscopic Study on High-k Dielectrics Based Nanoionics-Type ReRAM Structure under Bias Operation. ECS Transactions, 2014, 61, 301-310.	0.5	0
172	Direct Observation of Energy Distribution of Interface States at SiO2/4H-SiC Interface. ECS Transactions, 2016, 75, 207-211.	0.5	0
173	Hard X-Ray Photoelectron Spectroscopic Study on High-k Dielectrics Based Resistive Random Access Memory. ECS Transactions, 2017, 75, 39-47.	0.5	0
174	Study of Sn and Mg doping effects on TiO <sub>2</sub> /Ge stack structure by combinatorial synthesis. Japanese Journal of Applied Physics, 2018, 57, 04FJ04.	1.5	0
175	Near Surface Structures and the Electronic States of Polar InN. ECS Transactions, 2018, 86, 103-108.	0.5	0
176	Purpose of this Special IssueÂ: "Vacuum and Surface Science of Films― Vacuum and Surface Science, 2021, 64, 154-155.	0.1	0
177	Atomic Structures and Interface States Density at SiO <sub>2</sub> /4H-SiC Interface. Vacuum and Surface Science, 2021, 64, 312-317.	0.1	0
178	Vibrational Structure of Adsorbates As Revealed by High Resolution Core Level Photoelectron Spectra. Hyomen Kagaku, 2003, 24, 301-305.	0.0	0
179	Precursor Mediated Cycloaddition Reaction of Ethylene on Si(100)c(4*2). Hyomen Kagaku, 2005, 26, 474-479.	0.0	0
180	Direct Observation of Electronic States in Gate Stack Structures: XPS under Device Operation. ECS Meeting Abstracts, 2011, , .	0.0	0

#	Article	IF	CITATIONS
181	Direct Observation of the Energy Distribution of Interface States at SiO <sub>2</sub> /4H-SiC Interface: Operando Hard X-ray Photoelectron Spectroscopic Study. Hyomen Kagaku, 2017, 38, 347-350.	0.0	Ο
182	1 year study in Grenoble. Vacuum and Surface Science, 2018, 61, 813-814.	0.1	0
183	Chemical-state-discriminated hard X-ray photoelectron diffraction study for polar InN. Journal of Surface Analysis (Online), 2019, 26, 138-139.	0.1	0
184	Purpose of the Special IssueÂ: "Recent progress in Practical Surface Analysis― Vacuum and Surface Science, 2021, 64, 492-492.	0.1	0
185	Chemical States of Active and Inactive Dopant Sites in Si-doped GaN(0001). Vacuum and Surface Science, 2022, 65, 309-314.	0.1	0